

Recent Advances in Drug Release, Sensing, and Cellular Uptake of Ring-Opening Metathesis Polymerization (ROMP) Derived Poly(olefins)

Uppendar Reddy Gandra, Santhosh Kumar Podiyanachari, Hassan S. Bazzi,* and Mohammed Al-Hashimi*



Cite This: *ACS Omega* 2023, 8, 1724–1738



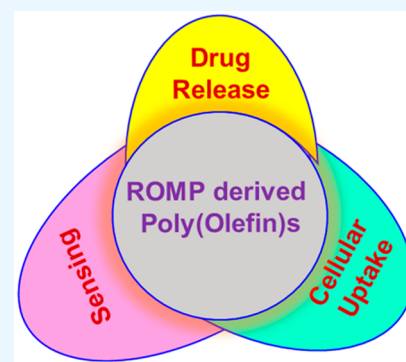
Read Online

ACCESS |

Metrics & More

Article Recommendations

ABSTRACT: The synthesis and applications of ring-opening metathesis polymerization (ROMP) derived poly(olefins) have emerged as an exciting area of great interest in the field of biomaterials science. The major focus of this mini-review is to present recent advances in the synthesis of functional materials using ROMP-derived poly(olefins) utilized for drug release, sensing, and cellular uptake in the past seven years (2015–2022). This review reveals that materials synthesized by ROMP-derived well-defined functional poly(olefins) stand to be highly promising systems for medical as well as biological studies. Thus, this review may prove to be beneficial for the design and development of new smart and flexible-functionality ROMP-based polymeric materials for various biological applications.



INTRODUCTION

Conventional polymeric materials such as plastics, artificial fibers, and rubber have gained much attention due to their ease of modification, chemical robustness, improved mechanical properties, and excellent stability.¹ There is a need for the rapid development of smart polymeric materials with unique features that enable advancement in the areas of sensing, bioimaging, energy-harvesting, and storage applications.¹ In this regard, functional polymeric materials have attracted wide attention, due to their potential in a broad range of applications.¹

Conventional methods such as oxidative coupling polymerization, electrochemical polymerization, and reversible addition–fragmentation chain transfer (RAFT) polymerization as well as atom transfer radical polymerization (ATRP) are well-known for the synthesis of conjugated functional polymeric materials. Among these conventional polymerization methods, catalytic ring-opening metathesis polymerization (ROMP) has become a remarkable polymerization technique for synthesizing a variety of functional polymers using various cycloalkene monomers (M1–M11) utilizing either the Schrock-type molybdenum (Mo)- or tungsten (W)-based metal alkylidenes 1 and 2² and Grubbs- or Hoveyda–Grubbs-type Ru alkylidenes olefin metathesis catalysts 3–7³ (Figure 1). A series of such functional poly(olefins) have been used to investigate their potentials in the area of supramolecular chemistry.⁴

Covalently bonded pendant optical recognition units on the poly(olefin) play an important role in constructing polymeric materials for sensing and drug delivery applications.⁵ There are several strategies to introduce optical recognition units such as fluorophores into ROMP-derived poly(olefins). In the most common approach, monomers can be attached with fluorophore molecules to synthesize fluorophore-functionalized homopolymers. In addition, copolymerization with various monomers can afford multifunctionalized copolymers with different side functional groups exhibiting various structural properties. A general schematic representation of ROMP for the synthesis of fluorophore-incorporated homo- and copolymers is outlined in Scheme 1a,b. Other strategies include postpolymerization, which is functionalized via ROMP on the double bond in the polymer backbone. In addition, the use of a fluorophore-appended carbenoid ligand on the initiator affords fluorophore-incorporated polymer chains.

By utilizing the ROMP technique, polymerization-induced self-assembly (PISA) has attracted much attention as a strategy to provide copolymers (mainly diblock) containing solvophi-

Received: August 29, 2022

Accepted: November 17, 2022

Published: January 3, 2023



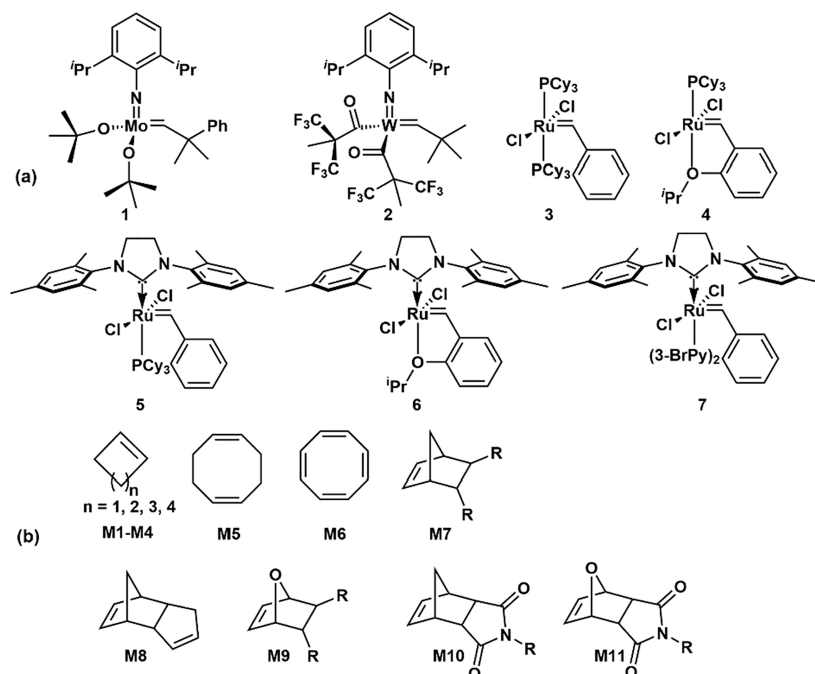
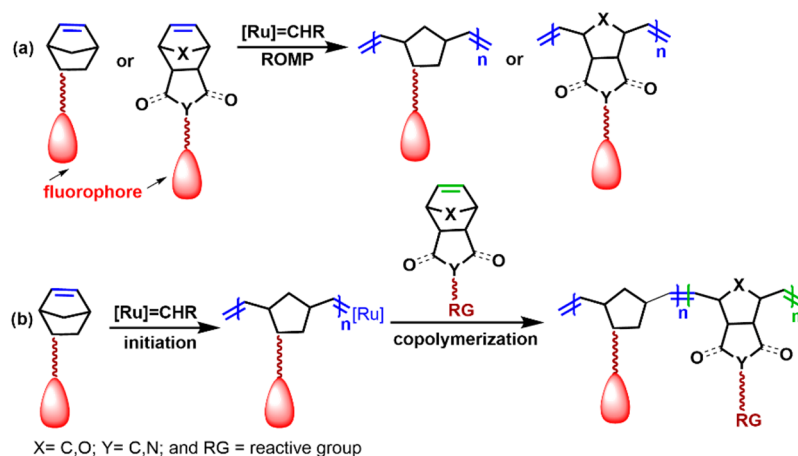


Figure 1. (a) Representative Mo- or W-based Schrock-type and Ru-based Grubbs- or Hoveyda–Grubbs-type alkylidene complexes and (b) various mono- and bicycloalkene monomers.

Scheme 1. General Schematic Representation of the ROMP of Fluorophore-Incorporated Cycloolefins: (a) Homopolymerization; (b) Copolymerization



philic functionalities with tailored compositions.⁶ The research groups of Gianneschi and Choi reported a series of examples of ring-opening metathesis polymerization induced self-assembly (ROMPISA) derived poly(olefins) using norbornene derivatives and investigated their self-assembled nanostructured behavior for biomedical and energy storage applications.⁷ These classes of polymers differ in their physicochemical properties in comparison with the polymers prepared by other conventional polymerization techniques. Most recent investigations have elucidated the significance of such self-assembled poly(olefins) in biomaterials and energy storage applications.

In this mini-review, we will cover the recent advances of ROMP-derived poly(olefins) and their various applications in the areas of sensing, drug release, and cellular uptake. In addition, an overview of the methodologies and strategies

utilized for the synthesis of such poly(olefins) by ROMP from 2015 to the present day will be described.

ROMP-DERIVED POLY(OLEFINS) FOR DRUG RELEASE

The use of functional poly(olefins) prepared via the ROMP approach for drug release and cellular uptake applications have not been much explored. In comparison to other drug carrier applications, polymeric nanoparticle-based drug delivery systems have received much attention because of their ability to release drugs directly to the specific site location as well as their facile functionalization with high quantities of the drug. In addition, the determination of the spatial distribution of the molecules and the low drug loading into the nanocarriers are key challenges. In this context, self-assembled amphiphilic polymeric nanomaterials have been widely used as promising

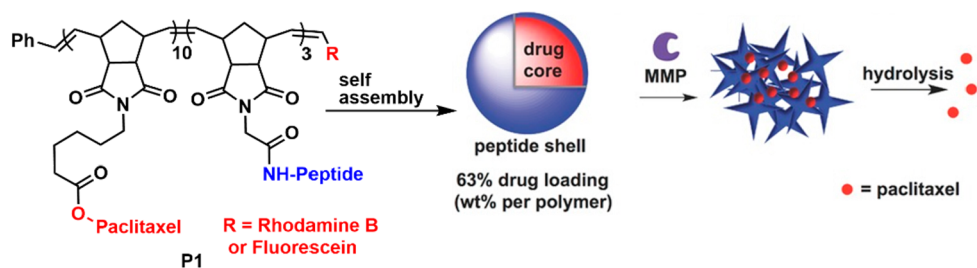


Figure 2. Enzyme-responsive and paclitaxel-conjugated diblock copolymer **P1**, self-assembled into polymer nanoparticles, and subsequent morphology change in response to MMP. Reprinted with permission from ref 9. Copyright 2015, John Wiley and Sons, Inc.

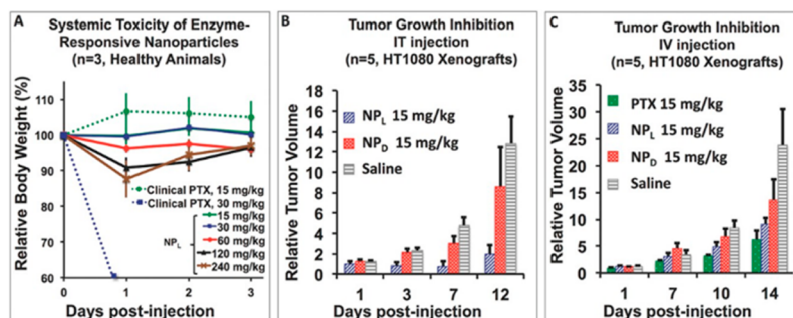


Figure 3. (a) Maximum tolerated dose (MTD) of IV injection, (b) tumor growth IT injection, and (c) tumor growth IV injection. Reprinted with permission from ref 9. Copyright 2015, John Wiley and Sons, Inc.

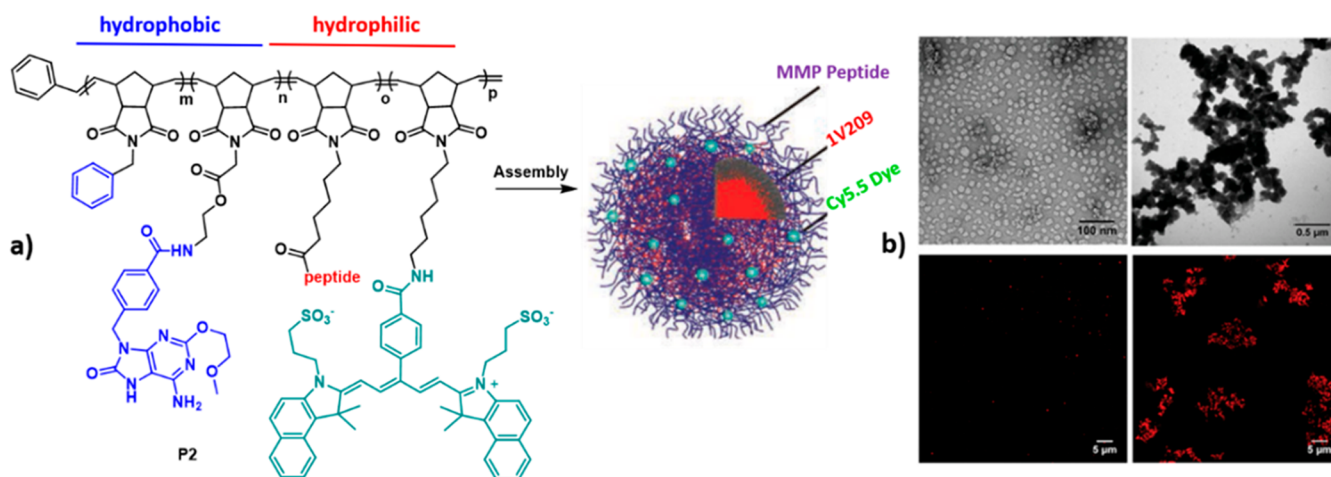


Figure 4. (a) Immune-therapeutics-loaded copolymer **P2** self-assembled into micelles and (b) morphological studies by TEM and SIM analysis. Reprinted with permission from ref 10. Copyright 2019, John Wiley and Sons, Inc.

delivery vehicles because of their high colloidal stability at low solution concentrations and biocompatibility. Aqueous polymerization-induced self-assembly (PISA) is a well-established procedure for the *in situ* synthesis of polymeric nanoparticles with tunable morphologies at high solid concentrations.⁸ The resulting polymeric nanoparticles/objects provide drug solubility and potential improvement in selectivity upon delivery to the target tissues.

In this area of research, Gianneschi and co-workers have reported the synthesis of the diblock graft copolymer **P1** via ROMP of a hydrophilic matrix metallo proteinase (MMP) responsive peptide monomer with directly polymerizable hydrophobic paclitaxel (PTX) moieties (Figure 2).⁹ PTX is well-known as a potent microtubule-stabilizing agent and is a standard component of chemotherapy regimens for many

malignant and metastatic cancers. In this study, the authors described the use of a PTX stabilizing agent, where the MMP is an enzyme, which makes the materials undergo a nano- to microscale change in size coupled with a change in morphology. As can be seen in **P1**, PTX was esterified through its 2'-OH group with a norbornenyl moiety to make it pliable to ROMP and rendering it into a fully inert prodrug material prior to the hydrolysis from the polymer support. In addition, to track the loaded drug polymeric **P1** materials *in vivo*, the authors introduced a Förster resonance energy transfer (FRET) pair of fluorophores such as fluorescein as a donor or rhodamine B as an acceptor in the terminal polymer chain. After copolymerization, the resultant drug-loaded copolymer **P1** was assembled into spherical nanoparticles bearing an MMP-responsive peptide-based nanoparticle shell.

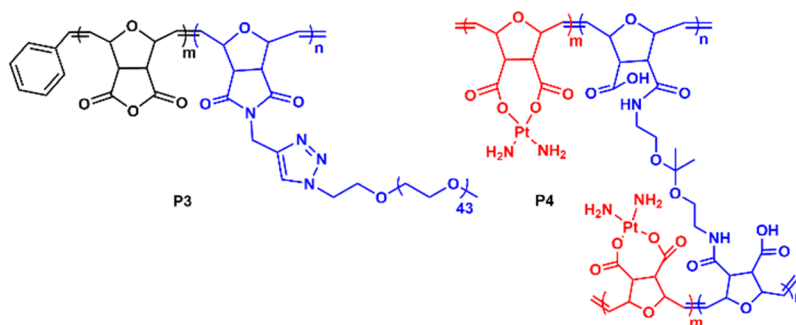


Figure 5. Self-assembled linear-brush polymer **P3** and *cis*-platinum-loaded acid degradable cross-linked polymer **P4** for the generation of acid-degradable cross-linked vesicles.

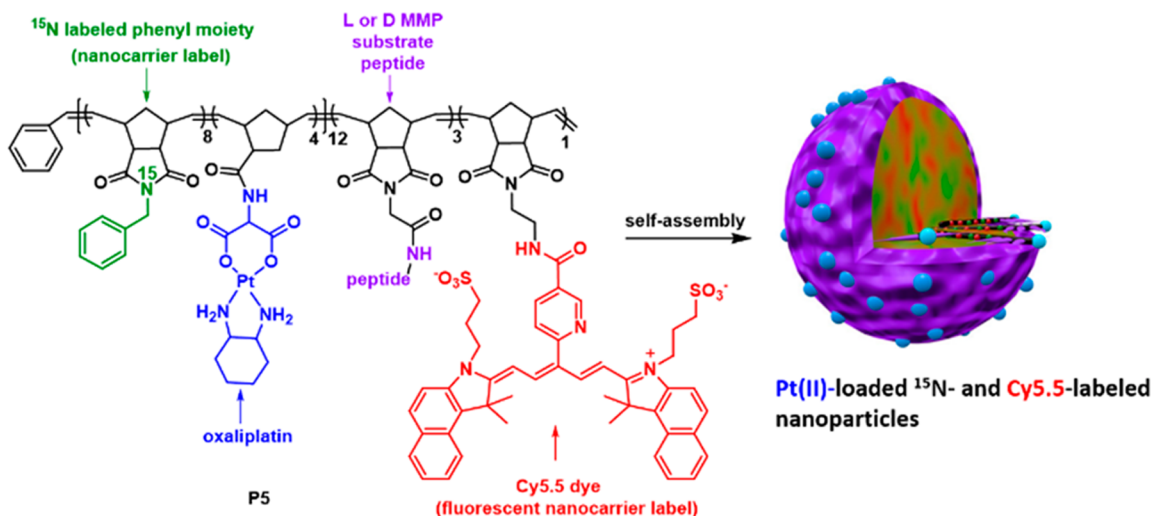


Figure 6. Pt(II)-loaded amphiphilic copolymer **P5** self-assembled nanoparticles. Reprinted with permission from ref 13. Copyright 2018, American Chemical Society.

Due to the MMP binding, the drug is shielded from the body until it reaches its specific target, allowing for the safe delivery of exceptionally high doses of chemotherapeutic PTX. In this work, the authors also examined the safety and efficiency of the PTX-loaded NPs as a proof of concept in *in vivo* studies: first the maximum tolerated dose (MTD) of IV injection and second the efficiency post-IT injection. For these studies authors utilized an HT-1080 fibrosarcoma xenograft cancer model known to overexpress MMPs and to rapidly proliferate in a predictable manner after the a subcutaneous implantation (Figure 3a–c). Another challenge in this study was the delivery of immune therapeutics into the specific tumor site location, and this was mainly because of the insufficient solubility, stability, and off-target delivery of immune stimulatory molecules that prevent their direct conversion as clinical therapeutics. In order to address these challenges, Gianneschi and co-workers reported disease-responsive polymer-**P2**-based nanocarriers that contained immune therapeutics inside the material (Figure 4a).¹⁰ The polymeric nanocarrier **P2** has been prepared from self-assembled amphiphilic diblock copolymers via ROMP of norbornene-derived monomers using the Grubbs third-generation catalyst 7.

The hydrophobic part of the block copolymer consists of Toll-like receptor 7 (TLR7) agonist 1V209 and the hydrophilic block copolymer part contains peptides as substrates of MMPs and Cy5 dye. The Cy5 fluorescent dye in the polymer chain was used for the *in vivo* imaging. In this work, the authors

described that under dialysis the aqueous solution of the copolymer **P2** was converted into a 15 nm size having spherical micelles and the subsequent exposure to MMP-9 resulted in the formation of immune stimulatory microscale assemblies. In addition, upon treatment of **P2**-based nanocarriers intravenously (IV) into mice bearing 4T1 breast cancer tumors, the reduction of primary tumor growth and inhibition of lung metastases was observed. The morphological changes were investigated using transmission electron microscopy (TEM) and structured illumination microscopy (SIM). As on the right-hand side of Figure 4b, the images illustrate the different morphologies of I-NPF before and after enzyme cleavage.

Among various transition-metal-incorporated drug-releasing materials, platinum-based drugs are some of the most effective medicines and are currently utilized to destroy the growth of many solid tumors, including bladder, ovarian, testicular, small-cell, and lung cancers. In comparison with the small conventional molecules, platinum analogues or platinum drug loaded polymeric nanoparticles or vesicles have notable advantages, such as an improved solubility of platinates that prolong their half-life in the body and thus increase their distribution into tumor sites.¹¹ Qiao and co-workers reported nontoxic and degradable ROMP-derived cross-linked polymeric vesicles as efficient pH-sensitive nanocarriers for the delivery of platinum drugs.¹² The polymeric vesicles were composed of the self-assembly of the linear-brush poly(oxanorbornene)-based diblock copolymer **P3** in acetone

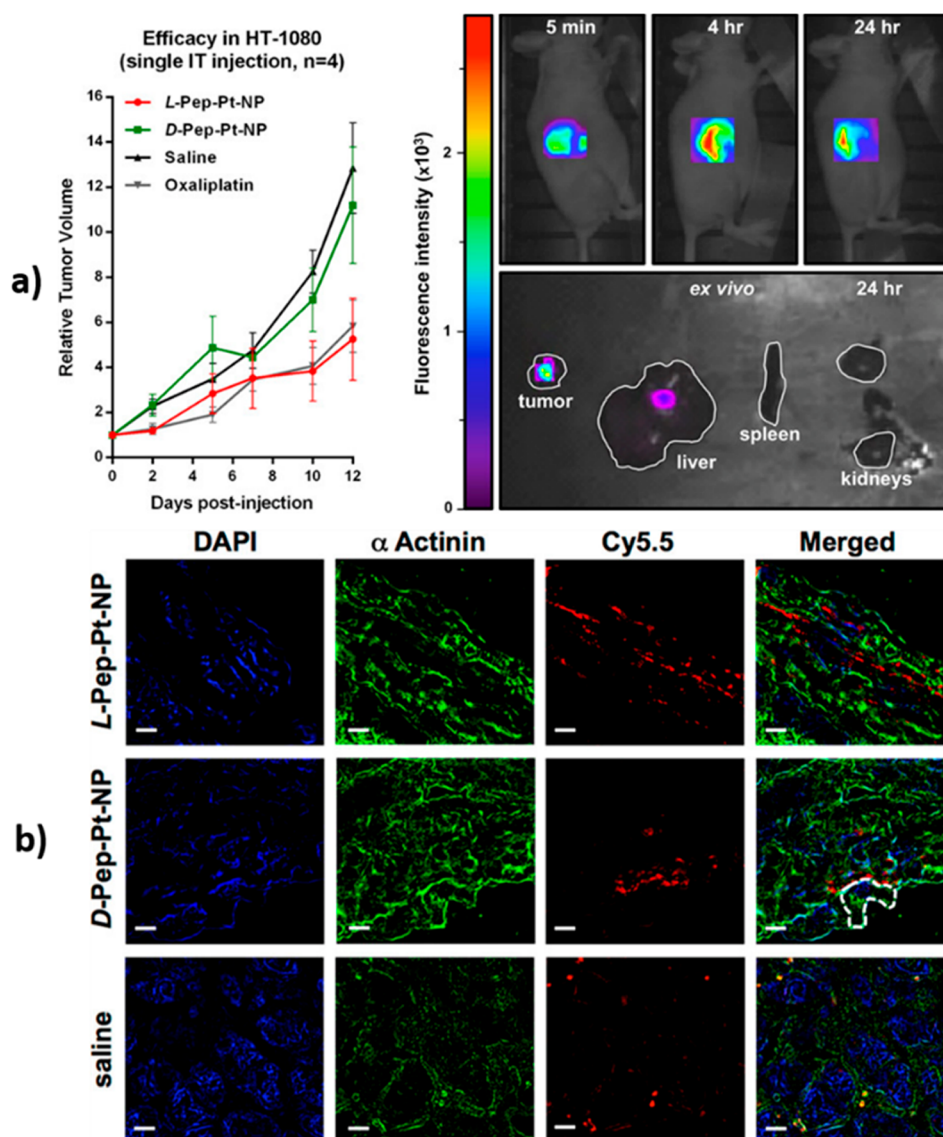


Figure 7. Efficacy of P5 with whole-animal and *ex vivo* organ targeting data. (a, top left) Comparison of L-Pep-Pt-NP to D-Pep-Pt-NP and oxaliplatin with respect to Pt and saline following IT injection. (a, top right) Time course of live-animal fluorescence imaging following IT injection of L-Pep-Pt-NP *ex vivo* tissue analysis as well as fluorescence imaging of tumor, liver, spleen, and kidney. (b) SIM imaging analysis. Reprinted with permission from ref 13. Copyright 2018, American Chemical Society.

followed by cross-linking between pendant anhydrides and diamino ketal cross-linker P4 (Figure 5). The hydrolyzed anhydrides of cross-linked polymeric vesicles led to the formation of diacid functionalities, which were subsequently implemented to conjugate cisplatin, and this was released from the drug-loaded cross-linked polymeric vesicles upon exposure to acidic conditions.

Gianneschi and co-workers also reported the capability of Pt(II)-loaded polymer P5 based nanoparticles for the enzyme-directed assembly of particle therapeutics (EDAPT).¹³ The EDAPT polymeric nanoparticles were generated through the assembly of ROMP-derived amphiphilic block copolymers, which were obtained from different cycloolefin monomers. The polymeric material was based on these monomers containing an analogue of the Pt(II)-incorporated drug oxaliplatin, and ¹⁵N-labeled monomer units were designed in the hydrophobic portion of the resultant polymer backbone along with a hydrophilic block having near-infrared cyanine

dye (Cy5) and a peptide linkage that was designated as a substrate for tumor metalloproteinase. Copolymerization of all these monomers resulted in the formation of amphiphilic block copolymer P5, and a subsequent dialysis in DMSO and water provided drug-loaded nanoparticles (Figure 6).

In addition to the synthesis of nanoparticles, the correlated optical and isotopic nanoscopy (COIN) method was utilized to determine the location of the drug carriers; this approach was used to generate materials with exceptionally high drug loadings and high concentrations of particles in solution. The authors also examined the ability of specific and selective delivery of Pt drugs to tumor tissues, while limiting off-target toxicity. It was reported that L-Pep-Pt-NP was able to inhibit tumor growth relative to both the saline and D-Pep-Pt-NP controls. In addition, the experiment was carried out using oxaliplatin, which suggested packaging of the Pt drug in a nanocarrier does not adversely affect its therapeutic potential (Figure 7a). A structural illumination microscopy (SIM)

imaging analysis was used by authors to determine thick tumor tissue sections of animals pretreated with L-Pep-Pt-NP (top), D-Pep-Pt-NP (middle), or saline (bottom) (Figure 7b) using specific fluorescent probes having various functionalities in the copolymers.

In another report, the same group described a one-pot aqueous-phase synthesis of structurally different cisplatin drug bound amphiphilic copolymer **P6** based micellar nanoparticles via ROMP using a ruthenium alkylidene initiator (Figure 8).¹⁴

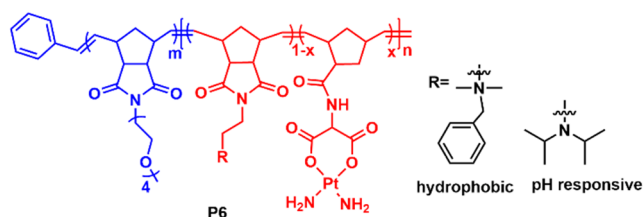


Figure 8. Structure of the amphiphilic copolymer **P6**.

The obtained polymer contained a poly(oligo-ethylene glycol) side-functional macro-stabilizer block, which was extended with a cisplatin analogue of a norbornene dicarboximide derivative using quaternary amine functionalities. In order to understand the pH effects, the authors introduced pH-responsive 2-(diisopropylamino)ethyl norbornene dicarboximide along the polymer chain and studied the effects of pH on the interactions with the cellular membrane and endosomes during *in vitro* delivery.

Similarly, Shunmugam and co-workers utilized the ROMP methodology to synthesize norbornene-based platinum conjugated copolymer **P7** for cancer therapy (Figure 9).¹⁵ The

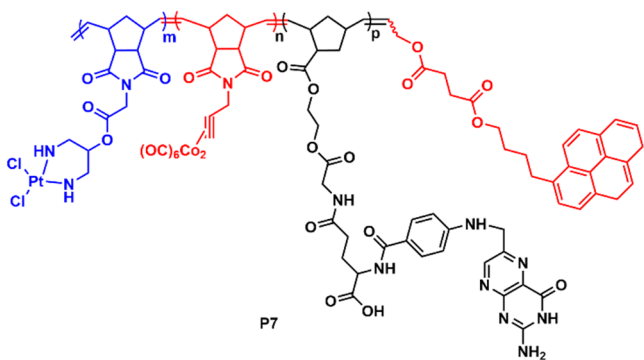


Figure 9. Polymer structure of **P7**.

authors introduced both cobalt carbonyl and pyrene groups in the polymeric chain to provide magnetic resonance imaging (MRI) capability and fluorescence imaging ability. The PEG-modified folic receptor moieties in the polymeric chain were selected for water solubility and site-specific therapy. The prodrug **P7** formed nanoaggregates in aqueous medium by stabilizing the hydrophobic segment in its core. It was observed that the nonaggression behavior of **P7** is more in HeLa and B16F10 cells with an improved antiproliferative effect in comparison to free cisplatin. In addition, it was described that the Pt drug was released upon addition of esterase to the nanoaggregate solutions of **P7**.

The precise spatial and temporal control over the release of CO is a major necessity for medical applications, especially CO as an important cell-signaling molecule for therapeutic

applications. Al-Hashimi and co-workers reported the first example of utilizing green-light-responsive CO-releasing polymer **P8** synthesized via ROMP (Figure 10).¹⁶ Poly-(norbornene)-based **P8** consists of di(2-picoyl)amine having an Mn(I) carbonyl core as a CO-releasing source conjugated to a naphthalimide fluorophore unit. The polymer **P8** was found to be highly stable under dark conditions and released CO under low-energy wavelength irradiation (550 nm, ≤ 28 mW). Upon irradiating a solution of **P8**, a bathochromic shift ($\lambda = 70$ nm) was observed in the absorption spectrum centered at 350 to 420 nm and a gradual increase in emission intensity at 530 nm was observed with time due to the release of CO molecules (Figure 10a,b). In addition, stretchable materials using polytetrafluoroethylene (PTFE) strips based on **P8** were fabricated to afford **P8**-PTFE. The amount of CO released from one strip (1.5 mg of **P8** loaded) under irradiation within 45 min was measured to be 45 ppm.

ROMP-DERIVED POLY(OLEFINS) FOR SENSING

The use of chemosensor-appended poly(olefins) for the sensing of various metal ions has not been much explored. In contrast with molecular sensors, polymer-based sensors have several advantages, such as (i) there would be a high signal amplification in the polymer-based system because of the increase in the number of receptor moieties attached to a polymer backbone site⁵ and (ii) the polymeric films are easily fabricated into devices. In addition, by incorporating various fluorophores and recognition units into the polymer backbone, one can produce an invaluable combination of different outputs (Scheme 2).⁴ Considering various polymer-based sensors, ROMP-derived poly(olefins) have attracted much attention due to their great advantages over conventional polymeric materials. Major advantages of ROMP-derived poly(olefins) such as high density of functional group tolerance, excellent stability and solubility, and narrow polydispersity indices, which provides the opportunity to synthesize block copolymers while allowing precise placement of the various chemosensor molecules in each block. In addition, these classes of polymers having covalent immobilization of chemosensors reduce fluorophore leaching, thereby improving sensor stability. Another intriguing feature of ROMP-derived poly(olefins) is that amorphous materials can be used for electroactive applications because of improved film-forming properties. Furthermore, ROMP-derived poly(olefin) backbones are virtually nonabsorbing to UV-vis irradiation, which makes them suitable systems for the polymerization of photoreactive or photochromic compounds.

In 1997, Buchmeiser and co-workers introduced a new material for solid-phase extraction (SPE) of metal ions for the first time using ROMP-derived polymers bearing pendant chelating moieties.¹⁷ However, systems that are appropriate for a selective metal ion extraction has not been much investigated since this last report. The selective detection of metal ions has great importance in the area of biochemical research, due to the metal ions playing an important role in living systems and in the environment. Among the heavy-metal ions, Hg^{2+} is one of the most potent neurotoxic metals and it deleteriously affects human life as well as plant physiology.¹⁸ Unlike Hg^{2+} , Cu^{2+} -based ions play an important role in biological processes in the human body. Therefore, the demand for the efficient detection of heavy-metal ions from their ores and waste streams is of immense importance.

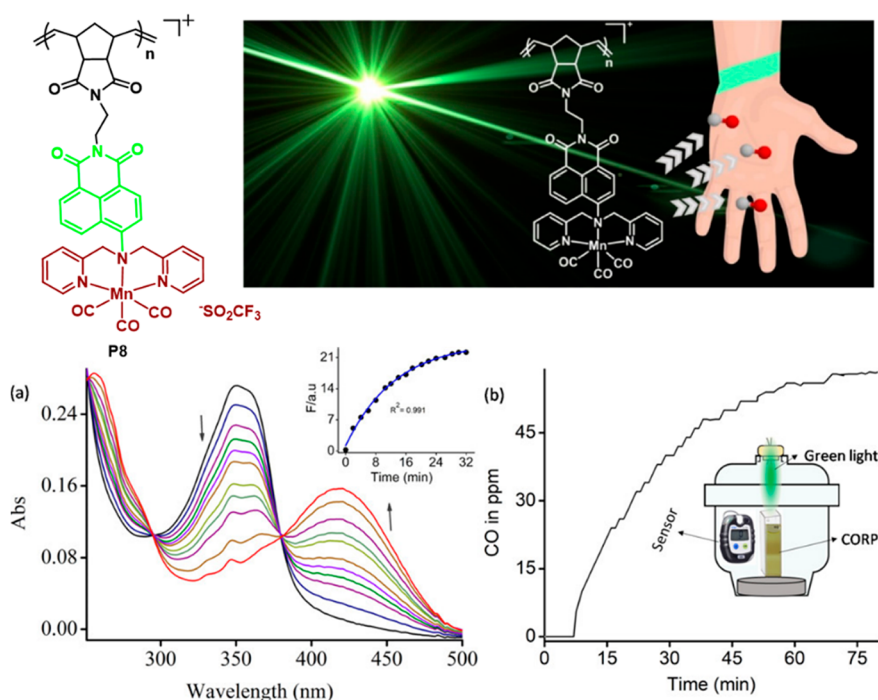
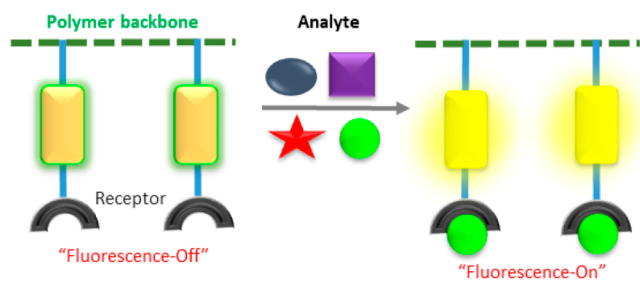


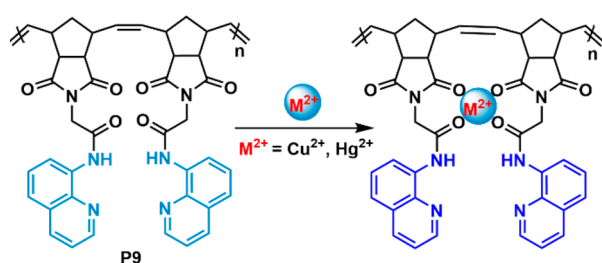
Figure 10. (top left) Structure of ROMP-derived polymer **P8**. (top right) Image representing the green-light-triggered CO release from polymer **P8**. (a, bottom left) Changes in the absorption spectra of **P8** under light irradiation. Inset: fluorescence intensity in the emission spectrum at $\lambda = 532$ nm following exposure to light vs time intervals. (b, bottom right) Amount of CO release from **P8**. Reprinted with permission from ref 16. Copyright 2019, American Chemical Society.

Scheme 2. Schematic Representation of a Chemosensor-Appended Polymer Backbone



In this area of research, Cao and co-workers developed the ROMP-derived quinolone-appended poly(norbornene) sensors **P9** using Grubbs' first-generation catalyst. The authors aimed to synthesize an imidic acid tautomeric binding mode of metal-ion-based polymer probes (Scheme 3).¹⁹ The obtained polymer probes exhibited fluorescence-off response in the absence of metal ions. However, UV-vis and emission titration experiments confirmed that **P9** is selective for Hg^{2+} and Cu^{2+}

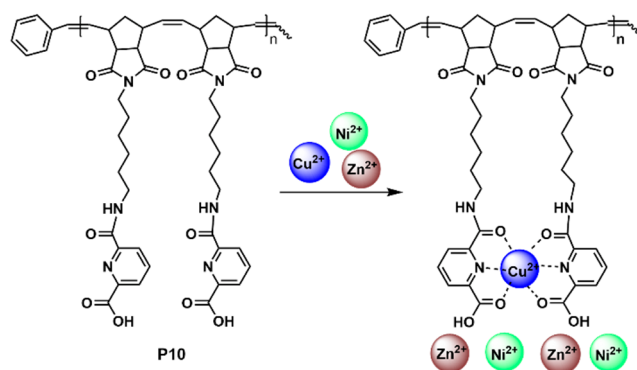
Scheme 3. Possible Binding Modes of **P9** with Metal Ions



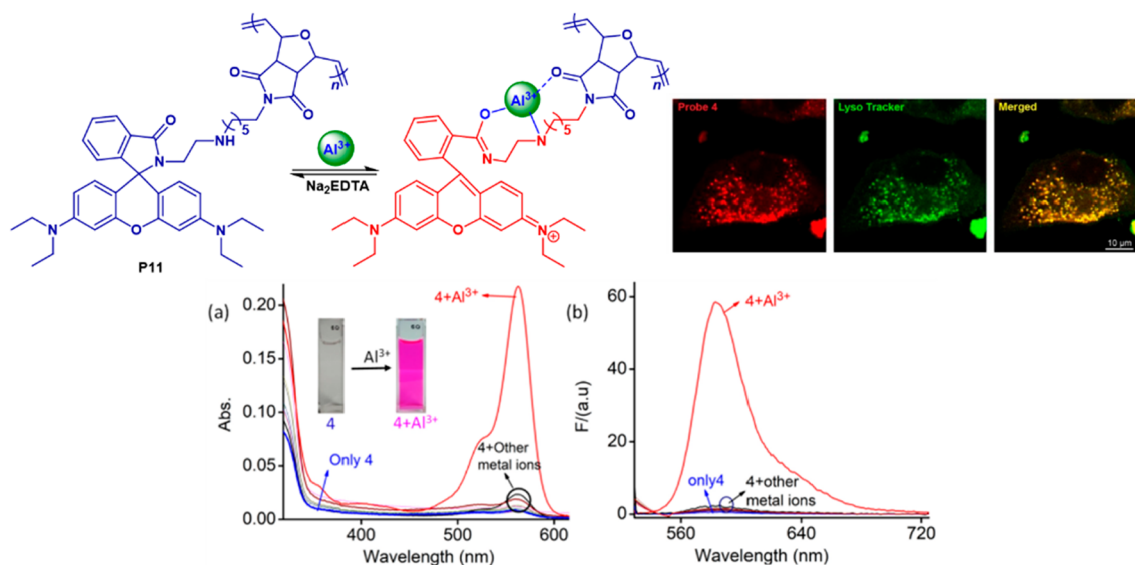
metal ions.¹⁹ The associated binding constants of **P9** with Hg^{2+} and Cu^{2+} characterized by fluorescence, NMR, and DFT calculation studies indicated that **P9** binds Hg^{2+} and Cu^{2+} in an imidic acid tautomeric form in CH_3CN solution, which exhibited a large emission enhancement response of **P9** at 416 nm.

The extractions of heavy-metal ions from aqueous solutions or their removal from wastewater is an extremely challenging process in many industrial applications as well as in environmental chemistry. Sessler and co-workers reported the synthesis of ROMP-derived polymer **P10** bearing pendant picolinic acid functionalities for the selective extraction of Cu^{2+} ions from solid-liquid waste (Scheme 4).²⁰ The monomer-containing norbornyl moiety is tethered to a picolinic acid functionality. **P10** and its corresponding monomer showed high selectivity for Cu^{2+} ions among a series of other divalent metal cations. **P10** was further used for the purification of Cu

Scheme 4. Selective Extraction of Cu^{2+} Ion by Polymer **P10**

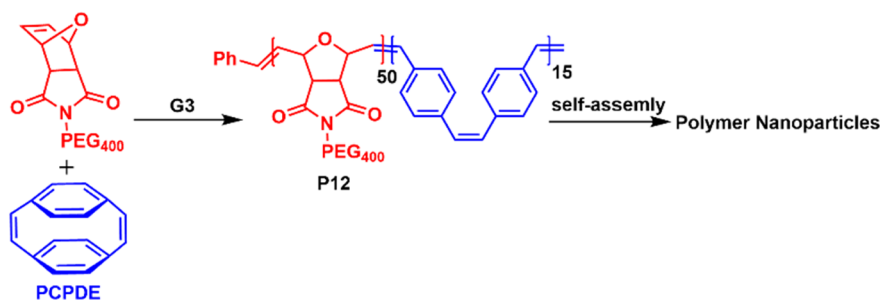


Scheme 5. (Top Left) Possible Binding Mechanisms of P11 with Al^{3+} Ions, (Top Right) Specific Labeling of P11 in Lysosomes, and Changes in (a) Absorption and (b) Emission Spectra of P11 in the Absence and the Presence of Different Metal Ions⁴



⁴ M^{n+} = Na^+ , K^+ , Mg^{2+} , Ca^{2+} , Ba^{2+} , Cu^{2+} , Ni^{2+} , Zn^{2+} , Cd^{2+} , Co^{2+} , Fe^{2+} , Cr^{3+} , Pb^{2+} , Al^{3+} , and Hg^{2+} in aqueous HEPES buffer–acetonitrile medium. Reprinted with permission from ref 21. Copyright 2020, Springer Nature.

Scheme 6. Polymer P12 for the Synthesis of Nanoparticles



radioisotopes. From these findings, the authors claimed that this technique can be very useful in the areas of hydrometallurgy and environmental cleanup.

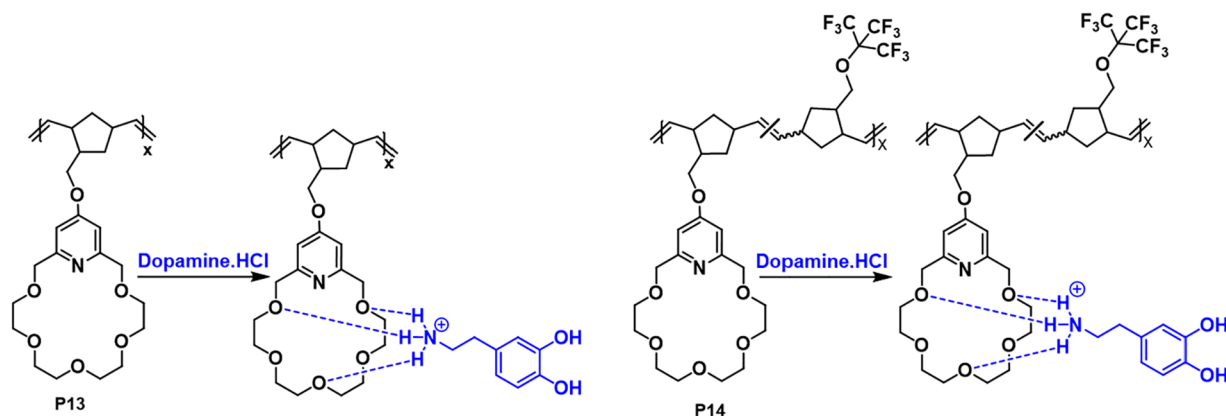
Similarly, Al-Hashimi and co-workers utilized the ROMP strategy to synthesize the rhodamine B appended poly-(norbornene)-based sensor **P11** for selective sensing of Al^{3+} ions (Scheme 5, top left).²¹ **P11** and its corresponding monomer displayed high selectivity for Al^{3+} ions among a series of other di- and trivalent metal cations. The polymer probe **P11** did not show any UV–vis or emission spectral band beyond 500 nm in the absence of any metal ion. However, UV–vis and emission titration experiments confirmed that **P11** is selective for Al^{3+} metal ions with reversibility. Polymer **P11** exhibited sharp changes in the electronic and emission spectra in the presence of Al^{3+} at $\lambda = 563$ and 584 nm, respectively (Scheme 5, bottom). Interestingly, the ROMP-derived **P11** specifically labels the lysosomes in cells even in the absence of Al^{3+} ions. Also, the authors utilized the pH sensitivity advantages of **P11** for the selective labeling of lysosomes (Scheme 5, top right).

The combination of conjugated block copolymers and their self-assembly is of considerable interest for various applications that include the studies on unfeasible nanostructures. Choi and co-workers reported a simple and efficient strategy for the one-

pot preparation of dimensionally controlled fluorescent nanostructures from ROMP-derived block copolymers for the detection of small-molecule nitroaromatics.²² The fluorescent poly(*p*-phenylenevinylene) block copolymer **P12** was synthesized via living ROMP of two different types of monomers such as norbornene derivatives for the soluble first block and unsubstituted [2.2]paracyclophane-1,9-diene (PCPDE) as an amplifying fluorescent monomer for the insoluble second block using Grubbs' third-generation catalyst 7 (Scheme 6).

Better nanocaterpillar morphology was observed for **P12** ($D_h = 135$ nm) in both chloroform and aqueous solutions for norbornene-tethered PEG-400:PCPDE with a feed ratio of 50:15. The sensing behavior of **P12** has been determined using neutral analytes such as 2,4-dinitrotoluene (DNT) and 2,4,6-trinitrotoluene (TNT). The UV–vis spectrum of **P12** showed an absorption maximum at 375 nm in chloroform, and the photoluminescence spectrum displayed an emission maximum at 491 nm with a quantum yield of 3.3%. Upon addition of 1 μM TNT to the solution of **P12**, there was a 40% decrease in fluorescent intensity and there were no significant changes observed in the UV–vis spectroscopy analysis. However, the lower detection limit of **P12** for TNT was determined to be 0.5 ppm.

Scheme 7. Proposed Noncovalent Interaction Mode between P13 and P14 with Dopamine HCl



On many occasions, supramolecular chemistry has been well used to evaluate reversible noncovalent bonding for the assembly of molecular architectures. Usually crown ethers (CEs) have been used as host molecules for various metal ions (K^+ , Na^+ , Ca^{2+} , and Mg^{2+}) for this purpose due to their larger cavities and great selectivities. Tuba and co-workers have reported excellent examples of such crown-ether-based host poly(olefins) via ruthenium alkylidene catalyzed ROMP using norbornene-functionalized pyridino-18-crown-6 ether monomer for the recognition of biogenic amines.²³ Among the synthesized polymers, homopolymer **P13** and the perfluoro-*tert*-butyl group-containing copolymer **P14** exhibited better supramolecular complexation with biogenic amines including dopamine and *L*-alanyl-*L*-lysine dipeptide via noncovalent interactions (Scheme 7). The detection of biogenic amines as well as binding studies with designed polymers was investigated by 1H NMR spectroscopy using a mixture of MeOD and CD_2Cl_2 in a ratio of 1:1 at 30 °C. With the aid of 1H NMR analysis, the biogenic amines were well identified due to the peak broadening in the region of 0.02–0.06 ppm that confirmed the supramolecular complex formation of pyridino-18-crown-6 ethers with protonated primary amines. In addition, theoretical calculations revealed the molecular switching of the crown-ether structure in **P14** bent to 90° from a planar structure upon $-NH_3^+$ ion coordination.

Similarly, Cao and co-workers also utilized the ROMP strategy to synthesize the pyrene-appended poly(norbornene)-based sensor **P15** for selective sensing of pyrophosphate (PPi) ions in 100% water solution (Figure 11a).²⁴ **P15** was obtained by ROMP using the Hoveyda–Grubbs second-generation catalyst **6**.²⁴ The polymer sensor consisted of sulfonamide, HN–, and triazolium donors for anion binding sites, and pyrene was used as a fluorescence unit. Under the excitation of **P15** at 360 nm the polymer displayed a strong pyrene-based excimer emission at 503 nm and weak monomer emission at 380 nm. Upon gradual addition of PPi to a solution of **P15**, the excimer emission at 503 nm decreased, and the monomer emission at 380 nm emerged to become the dominant peak. At the biological and bioanalytical application level, **P15** was successfully applied to monitor intracellular PPi in HeLa cells to detect the amount of PPi generated during the polymerase chain reaction. Very recently, the same group reported another pyrene-appended poly(norbornene), **P16**, for sequential detection of Hg^{2+} and biothiols (Figure 11a).²⁵ The corresponding monomer of polymer **P16** showed a strong pyrene moiety emission at 384 nm, while **P16** exhibited a

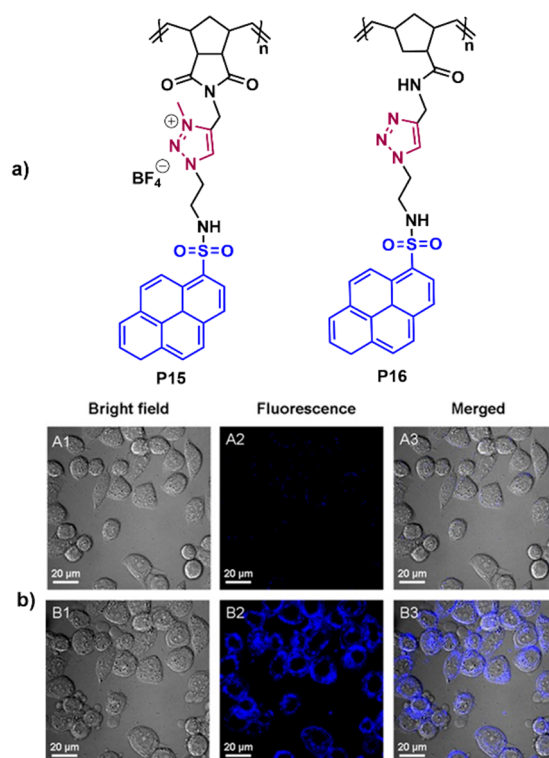


Figure 11. (a) Structure of ROMP-derived homopolymers **P15** and **P16**. (b) Confocal fluorescence images of HeLa cells incubated with **P15** (A1–A3 and B1–B3). Reprinted with permission from ref 24. Copyright 2016, Wiley-VCH.

similar range of monomer emission at 384 nm and a weak excimer emission centered at 490 nm, which could originate from the π – π stacking of the adjacent pyrene units of polymer **P16**. Upon addition of $Hg(II)$ to the solution of **P16** there was a decrease of the pyrene moiety emission at 384 nm and an increase in the the emission at 490 nm. The reverse phenomenon was observed for **P16** $Hg(II)$ upon the addition of biothiols. Furthermore, **P15** was utilized for the intracellular detection of pyrophosphate (PPi) in HeLa cells. The HeLa cells incubated with **P15** (20 μm) for 30 min at 37 °C displayed a weak blue fluorescence (A2). However, upon the addition of exogenous PPi to the cells with incubation for 10 min at 37 °C, the cells exhibited a highly intense blue fluorescence color (B2). This indicated that the polymer **P15**

Scheme 8. (a) Sensing Behavior of P17 and P18 in the Presence of Dichloroethyl Phosphate (DCP) and (b) Molecular Structures of P19 and P20, Respectively, for Di- and Triblock Copolymers

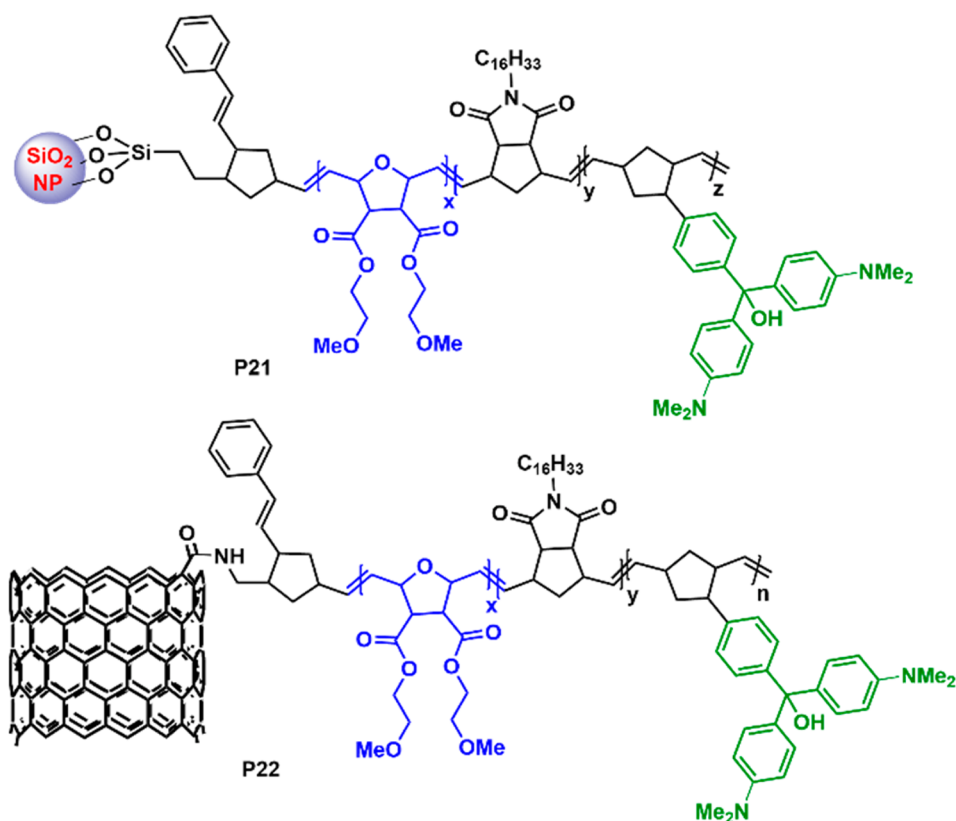
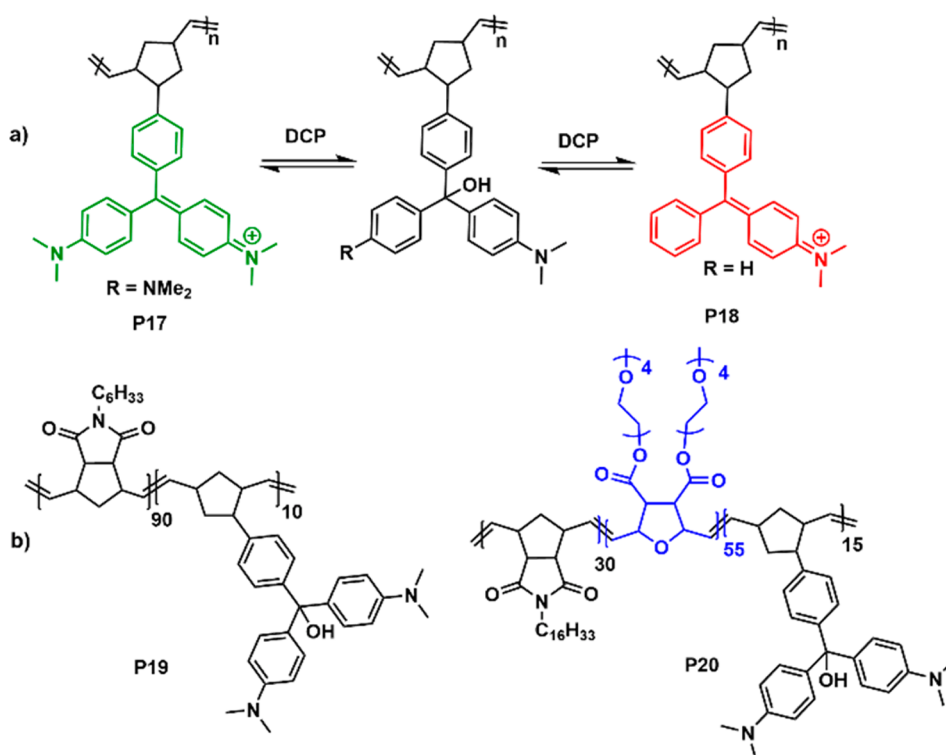


Figure 12. Grafting CWA-responsive copolymers P21 and P22 from nanoparticle-norbornene as well as CNT-norbornene via ROMP.

is able to enter HeLa cells and can detect PPI in living systems (Figure 11b).

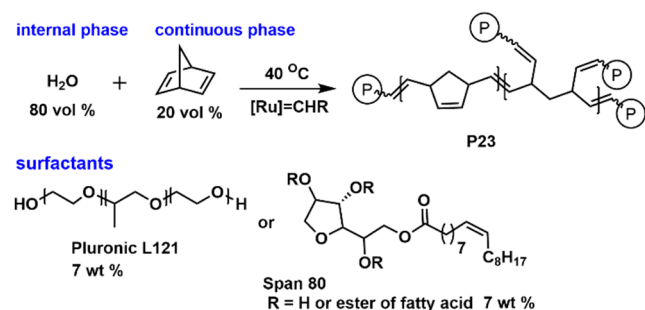
Chemical warfare agents (CWAs) such as tabun (GA), sarin (GB), soman (GD) and cyclosarin (GF) are known to be the

most significant dangers in the homeland as well as on the battlefield. CWA-responsive units are incorporated into polymers, and the resultant polymeric materials are more robust from an application point of view. In the area of this research, Swager and co-workers reported a series of polymeric materials that exhibited colorimetric responses upon exposure to CWA and incorporated them into a versatile detection platform based on copolymers that were synthesized via ROMP.²⁶ The triarylmethanol groups were incorporated into norbornene derivatives, and the subsequent ROMP reaction yielded different homopolymers **P17** and **P18** (Scheme 8a) and di- and triblock copolymers **P19** and **P20** (Scheme 8b). CWAs were incorporated into these tertiary alcohols appended polymers and displayed excellent reactivity and rapid colorimetric responses due to subsequent ionization followed by phosphorylation of the hydroxyl moiety. In addition, these polymers showed fully reversible responses toward diethyl chlorophosphate (DCP) in the presence of ammonium hydroxide vapor.

In another report, the same group proposed the design and synthesis of the hybrid polymeric nanoparticle-based **P21** by grafting a CWA-responsive polymer from a silicon dioxide surface synthesized using ROMP methodology (Figure 12).²⁷ It was found that the hydrodynamic radius of polymer-grafted SiO₂ nanoparticles decreased and the polymer chains collapsed upon exposure to CWA simulants. Very recently, the same group reported the ROMP-derived synthesis of the single-walled carbon nanotube (SWNT) functionalized CWA responsive polymer **P22** (Figure 12).²⁸ The obtained SWNTs were found to be vertically oriented nanopores spanning the membrane thickness, and the adoption of smaller diameter SWNTs increases upon the membrane breathability. In addition, these polymeric membranes can rapidly, selectively, and reversibly transfer from a highly breathable state in a safe environment to a chemically protective state with colorimetric response when exposed to CWA threats.

The extraction or removal of oxygen is an important process in food conservation to maintain the product safety and shelf life of goods. In this regard, oxygen scavengers are industrially significant in maintaining food product quality. Slugovc and co-workers reported an example for the first time of the polymeric material **P23** for organic oxygen removal using the ROMP strategy (Scheme 9).²⁹ The macroporous poly(norbornadiene) foams were made by curing high internal phase emulsions of norbornadiene in water via ROMP using appropriate amounts of a nonionic surfactant, either Pluronic L121 or Span 80, as emulsifying agents. A scanning electron

Scheme 9. Formulation of the High Internal Phase Emulsions (HIPEs) and Schematic Representation of the Structure of P23



microscope (SEM) analysis revealed that Span 80 produced structurally better defined foams than Pluronic L121.

The average oxygen uptake capacity has a rate of more than 300 mg of O₂ per 1 g of foam, and the polymeric **P23** foams quickly turn to yellow from white upon uptake of oxygen due to their fast oxidation in air under ambient conditions.

ROMP-DERIVED POLY(OLEFINS) FOR CELLULAR UPTAKE

Efficient cellular uptake is one of the key factors for regulating the biological activity of molecules, and it is often determined by the interactions between the molecule and the plasma membrane. Molecules that can readily cross over cell membranes are very essential in biomedical applications. The plasma membrane is the first barrier that prevents direct translocation of chemic entities and thus obstructs their efficient intracellular delivery.³⁰ Hydrophilic small-molecule drugs have poor permeability that reduces bioavailability and thus limits clinical applications. Also, the cellular uptake of macromolecules and drug carriers is very inefficient without any external assistance. Therefore, it is desirable to develop potent delivery systems to achieve an effective intracellular uptake of chemic entities. Amino acid and peptide based polymers have good biocompatibility as well as biodegradability; thus these classes of polymers are capable of diverse medicinal and diagnostic applications.^{7,31} However, certain types of peptide based therapeutic and diagnostic agents have limited applications, due to technical reasons such as errant proteolysis, inefficiencies in cellular uptake, and size-dependent renal clearance.³²

Gianneschi and co-workers have addressed these limitations by packing peptides into highly dense brush polymers **P24** via grafting-through ROMP of the peptide-based cycloolefin monomers (Figure 13).³³ This strategy provided polymeric structures that were resistant to proteolytic degradation without changing the chemical modification of the primary amino acid sequence in the peptide. The peptide brush copolymers **P24** were generated through ROMP of different norbornene-tethered substituents. To ensure solubility, polymers were prepared as block copolymers with a second block containing an oligo ethylene glycol (OEG) unit. Fluorescein molecules were introduced into polymer terminals to track cellular studies. In addition, two different therapeutic peptides such as GSGSG and KLA **P25** were chosen to demonstrate whether such peptides could penetrate cells upon polymerization (Figure 13). The peptide polymer **P24** was calibrated to be a resistant material to proteolytic degradation and cell penetration. In addition, no cytotoxicity was exhibited by any of these materials at concentrations up to 1 mM. The flow cytometry data displayed in Figure 14a shows the fluorescent signatures of HeLa cells treated with the polymers ($m \approx 60$) and their monomeric counterparts. The R control is a block copolymer that contains a single Arg attached via a short linker to each polymer side chain of this first polymer block ($m \approx 60$). The terminology “Flu” represents the fluorescein end label shown in **P24**. Also, the live-cell confocal microscopy images displayed in Figure 14b represent the average intensities from six consecutive 1 μm slices of HeLa cells treated with peptides and polymers ($m \approx 60$).

In another report, the same group expanded this platform to develop various ROMP-derived polymer brushes harboring pendant cell-penetrating peptides (CPPs), which were resistant to proteolysis and also had a cell penetration activity.³⁴ The

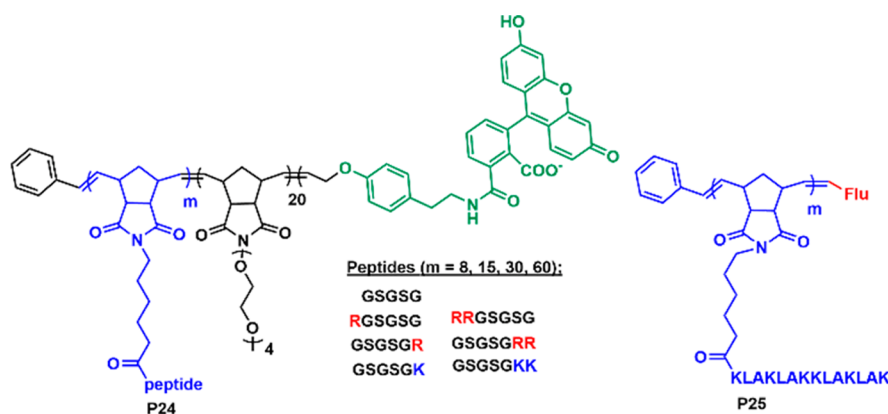


Figure 13. Cellular internalization of GSGSG-incorporated copolymer P24 and KLA peptide based homopolymer P25.

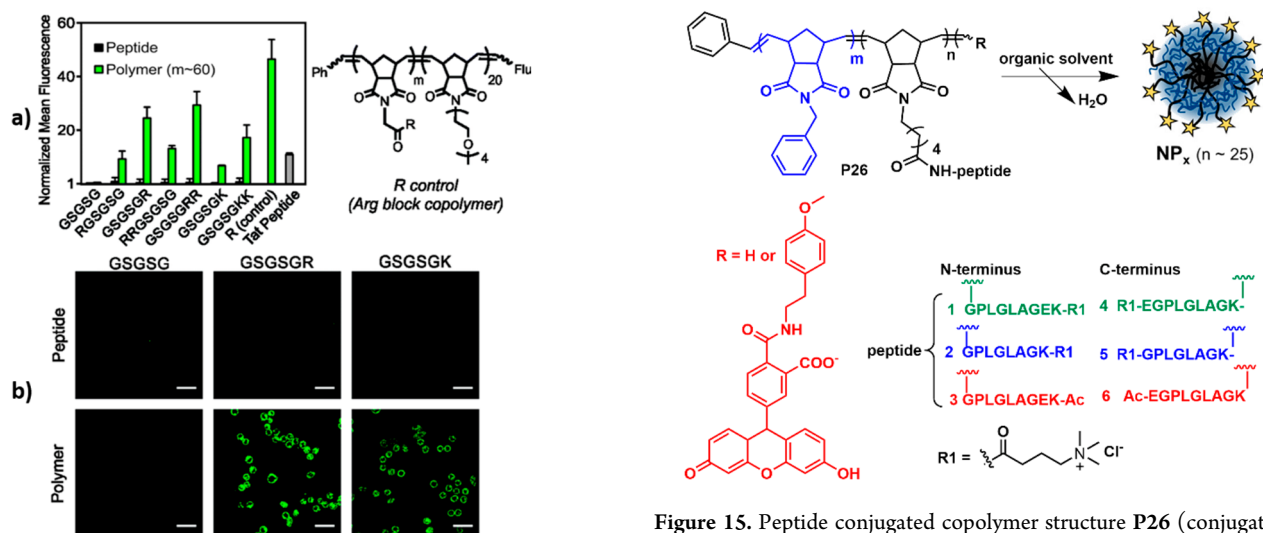


Figure 14. (a) Flow cytometry data displaying fluorescent signatures of HeLa cells treated with the polymers ($m \approx 60$) and their monomeric counterparts. The R control is a block copolymer that contains a single Arg attached via a short linker to each polymer side chain of this first polymer block. “Flu” is the fluorescein end label present in P24. (b) Live-cell confocal microscopy images showing the average intensities from six consecutive $1 \mu\text{m}$ slices of HeLa cells treated with peptides and polymers ($m \approx 60$). Reprinted with permission from ref 33. Copyright 2016, Royal Society of Chemistry.

elegant use of ROMP methodology has also allowed for the facile synthesis of graft-copolymer architecture P26, which is highly useful as a unique nanoparticle material for fluorescence imaging and also for either the evasion or uptake of macrophages (Figure 15).

SUMMARY AND OUTLOOK

In this review we have highlighted the recent advances in biomaterial applications of various ROMP-derived poly(olefins). The applications were described in detail with specific examples of poly(olefins) in the following subcategories. (i) Drug release: this category was described with a series of ROMP-derived self-assembled amphiphilic polymeric nanomaterials and their evaluations in drug releasing capability as promising delivery vehicles. (ii) Sensing: elucidation of a vast exploration of the ROMP-derived synthesis and advantages of polymer-based sensors and their performance studies in comparison with small organic probes. (iii) Cellular uptake:

Figure 15. Peptide conjugated copolymer structure P26 (conjugation to the N-terminus or ϵ -amino group of a C-terminal lysine residue of the peptide). Reprinted with permission from ref 34. Copyright 2017, American Chemical Society.

this was focused on describing the potential of bunch ROMP-induced self-assembled amphiphilic poly(olefins) in cellular uptake therapeutic applications. We envision that the recent advancements outlined in this review will provide an outlook on the design and the development of new ROMP-derived functional poly(olefins) for various biomaterials applications based on previously developed strategies. The challenges involve the design of novel functional cycloolefin monomers and ROMP of those monomers in a size- or length-controlled manner. In addition, a deeper understanding of structure–property relationships will allow a prediction of the performance of new poly(olefins) in the self-assembly or closely related structural behaviors. Recent advancements outlined in this mini-review will allow the reader to develop next-generation smart and flexible ROMP-based functional polymeric materials that can be used for various biological applications.

AUTHOR INFORMATION

Corresponding Authors

Hassan S. Bazzi – Division of Arts and Sciences, Texas A&M University at Qatar, Doha 23874, Qatar; Department of Materials Science & Engineering, Texas A&M University, College Station, Texas 77843-3003, United States; Email: bazzi@tamu.edu

Mohammed Al-Hashimi – *Division of Arts and Sciences, Texas A&M University at Qatar, Doha 23874, Qatar;*
orcid.org/0000-0001-6015-2178; Email: mohammed.al-hashimi@tamu.edu

Authors

Upendar Reddy Gandra – *Division of Arts and Sciences, Texas A&M University at Qatar, Doha 23874, Qatar;*
Department of Chemistry, Ulsan National Institute of Science and Technology (UNIST), Ulsan 44919, Republic of Korea;
orcid.org/0000-0002-7157-9668

Santhosh Kumar Podiyanchari – *Division of Arts and Sciences, Texas A&M University at Qatar, Doha 23874, Qatar*

Complete contact information is available at:
<https://pubs.acs.org/10.1021/acsomega.2c05563>

Author Contributions

All authors have given approval to the final version of the manuscript.

Notes

The authors declare no competing financial interest.

Biographies



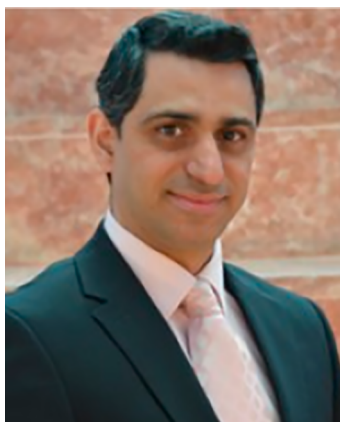
Upendar Reddy Gandra obtained his Ph.D. in Chemical Sciences under the supervision of Dr. Amitava Das from the CSIR-National Chemical Laboratory in 2016. After a first postdoctoral research (August 2015 to March 2018) with Prof. Alexander Schiller at the Friedrich Schiller University, Jena, Germany, he joined the Texas A&M University at Qatar (TAMUQ) with Prof. Hassan S. Bazzi in May 2018. At TAMUQ, his research focused on olefin metathesis derived functional polyolefins for sensing and drug release at the interface between supramolecular chemistry and medicine. After postdoctoral research at the TAMUQ, he moved to the Ulsan National Institute of Science and Technology (UNIST) in South Korea in December 2021. At UNIST, his research focused on organelle targeted self-assembly and supramolecular polymerization for drug-free cancer research as well as developing novel photosensitizers for photodynamic therapy (PDT) applications.



Santhosh Kumar Podiyanchari received his M.Sc. degree in 2003 from Mahatma Gandhi University. After working as a scientist at Jubilant Biosys Ltd, India, he was a doctoral student in the research group of Prof. Michael R. Buchmeiser at the Institute of Surface Modifications (IOM), Leipzig. He received his Ph.D. degree in olefin metathesis chemistry in 2010 from University of Leipzig. After his first postdoctoral research (2010–2014) in the group of Prof. Gerhard Erker at the University of Muenster, he spent two years (2015–2017) at Emory University in Atlanta within the group of Prof. Cora E. MacBeth and one year at the University of Amsterdam in the group of Prof. Bas de Bruin as Research Associate. Since 2018, he has been working as a research associate in the group of Prof. Hassan S. Bazzi at the Texas A&M University at Qatar. His research deals mainly with transition-metal-catalyzed olefin metathesis polymerizations and the study of macromolecular architectures.



Hassan S. Bazzi is the Senior Associate Dean for Research and Professor of Chemistry at Texas A&M University at Qatar. Dr. Bazzi received his Bachelor's and Master's degrees in Chemistry and Organic Chemistry, respectively, from the American University of Beirut (1996 and 1998) and his Ph.D. in Polymer Chemistry from McGill University (2003). He worked briefly with the United Nations as a chemical weapons inspector in Iraq before joining the Université de Montréal as a postdoctoral research fellow. He joined Texas A&M at Qatar as Assistant Professor in 2004 and was promoted to Associate Professor in 2009 and to Full Professor in 2014. Dr. Bazzi's research interests focus on olefin metathesis chemistry, polymer-supported catalysis, and homogeneous metathesis polymerization by ruthenium alkylidenes.



Mohammed Al-Hashimi received his MSci Honors degree in Pharmaceutical Chemistry in 2003, followed by a Ph.D. in 2007, from Queen Mary University of London. He subsequently worked as a Senior Development Chemist at Evotec, Oxfordshire, and later joined the Chemistry department at Imperial College London as a postdoc in 2008. Before joining TAMUQ in 2013, Al-Hashimi in 2012 worked at Qatar University as an Assistant Professor. He is a recipient of the Donald C. Bradley Prize, the ASPIC Prize, the Lefevre Prize, the ACMME Research Prize, and the Best Research Presentation Award in Energy and Environment Pillar ARC16. Most recently, he was awarded the TAMUQ Faculty Research Excellence Award and was named a Fellow of the Royal Society of Chemistry (FRSC). Al-Hashimi's research focuses on the synthesis of organic polymers, particularly the design and synthesis of organic semiconductor materials for a range of optoelectronic applications, including field-effect transistors, photovoltaic devices, and light-emitting diodes and sensors. His interests also include the synthesis of recoverable, reusable homogeneous and heterogeneous catalysts.

REFERENCES

- (1) Zhao, F.; Shi, Y.; Pan, L.; Yu, G. Multifunctional nanostructured conductive polymer gels: synthesis, properties, and applications. *Accounts of chemical research* **2017**, *50* (7), 1734–1743.
- (2) Schrock, R. R.; Hoveyda, A. H. Molybdenum and tungsten imido alkylidene complexes as efficient olefin-metathesis catalysts. *Angew. Chem., Int. Ed.* **2003**, *42* (38), 4592–4633.
- (3) Yasir, M.; Liu, P.; Tennie, I. K.; Kilbinger, A. F. Catalytic living ring-opening metathesis polymerization with Grubbs' second- and third-generation catalysts. *Nat. Chem.* **2019**, *11* (5), 488–494.
- (4) Breul, A. M.; Hager, M. D.; Schubert, U. S. Fluorescent monomers as building blocks for dye labeled polymers: synthesis and application in energy conversion, biolabeling and sensors. *Chem. Soc. Rev.* **2013**, *42* (12), 5366–5407.
- (5) Kim, H. N.; Guo, Z.; Zhu, W.; Yoon, J.; Tian, H. Recent progress on polymer-based fluorescent and colorimetric chemosensors. *Chem. Soc. Rev.* **2011**, *40* (1), 79–93.
- (6) Sankaran, N.; Rys, A. Z.; Nassif, R.; Nayak, M. K.; Metera, K.; Chen, B.; Bazzi, H. S.; Sleiman, H. F. Ring-opening metathesis polymers for biodetection and signal amplification: synthesis and self-assembly. *Macromolecules* **2010**, *43* (13), 5530–5537.
- (7) Callmann, C. E.; Thompson, M. P.; Gianneschi, N. C. Poly (peptide): synthesis, structure, and function of peptide–polymer amphiphiles and protein-like polymers. *Accounts of chemical research* **2020**, *53* (2), 400–413.
- (8) Foster, J. C.; Grocott, M. C.; Arkinstall, L. A.; Varlas, S.; Redding, M. J.; Grayson, S. M.; O'Reilly, R. K. It is Better with Salt: Aqueous Ring-Opening Metathesis Polymerization at Neutral pH. *J. Am. Chem. Soc.* **2020**, *142* (32), 13878–13885.
- (9) Callmann, C. E.; Barback, C. V.; Thompson, M. P.; Hall, D. J.; Mattrey, R. F.; Gianneschi, N. C. Therapeutic enzyme-responsive nanoparticles for targeted delivery and accumulation in tumors. *Advanced materials* **2015**, *27* (31), 4611–4615.
- (10) Battistella, C.; Callmann, C. E.; Thompson, M. P.; Yao, S.; Yeldandi, A. V.; Hayashi, T.; Carson, D. A.; Gianneschi, N. C. Delivery of Immunotherapeutic Nanoparticles to Tumors via Enzyme-Directed Assembly. *Adv. Healthc. Mater.* **2019**, *8* (23), 1901105.
- (11) Oberoi, H. S.; Nukolova, N. V.; Kabanov, A. V.; Bronich, T. K. Nanocarriers for delivery of platinum anticancer drugs. *Advanced drug delivery reviews* **2013**, *65* (13–14), 1667–1685.
- (12) Fu, Q.; Xu, J.; Ladewig, K.; Henderson, T. M. A.; Qiao, G. G. Degradable cross-linked polymer vesicles for the efficient delivery of platinum drugs. *Polym. Chem.* **2015**, *6* (1), 35–43.
- (13) Proetto, M. T.; Callmann, C. E.; Cliff, J.; Szymanski, C. J.; Hu, D.; Howell, S. B.; Evans, J. E.; Orr, G.; Gianneschi, N. C. Tumor Retention of Enzyme-Responsive Pt(II) Drug-Loaded Nanoparticles Imaged by Nanoscale Secondary Ion Mass Spectrometry and Fluorescence Microscopy. *ACS Central Science* **2018**, *4* (11), 1477–1484.
- (14) Wright, D. B.; Proetto, M. T.; Touve, M. A.; Gianneschi, N. C. Ring-opening metathesis polymerization-induced self-assembly (ROMPISA) of a cisplatin analogue for high drug-loaded nanoparticles. *Polym. Chem.* **2019**, *10* (23), 2996–3000.
- (15) Mukherjee, S.; Patra, D.; Dash, T. K.; Chakraborty, I.; Bhattacharyya, R.; Senapati, S.; Shunmugam, R. Design and synthesis of a dual imageable theranostic platinum prodrug for efficient cancer therapy. *Polym. Chem.* **2019**, *10* (23), 3066–3078.
- (16) Gandra, U. R.; Sinopoli, A.; Moncho, S.; NandaKumar, M.; Ninković, D. B.; Zarić, S. D.; Sohail, M.; Al-Meer, S.; Brothers, E. N.; Mazloum, N. A.; Al-Hashimi, M.; Bazzi, H. S. Green Light-Responsive CO-Releasing Polymeric Materials Derived from Ring-Opening Metathesis Polymerization. *ACS Appl. Mater. Interfaces* **2019**, *11* (37), 34376–34384.
- (17) Buchmeiser, M. R.; Atzl, N.; Bonn, G. K. Ring-opening-metathesis polymerization for the preparation of carboxylic-acid-functionalized, high-capacity polymers for use in separation techniques. *J. Am. Chem. Soc.* **1997**, *119* (39), 9166–9174.
- (18) Hu, W.; Wang, J. Design, synthesis and evaluation of liver-targeting fluorescent probes for detecting mercury ions. *Dalton Transactions* **2022**, *51* (29), 11005–11012.
- (19) Yao, P.-S.; Cao, Q.-Y.; Peng, R.-P.; Liu, J.-H. Quinoline-functionalized norbornene for fluorescence recognition of metal ions. *J. Photochem. Photobiol., A* **2015**, *305*, 11–18.
- (20) Fimognari, R.; Cinninger, L. M.; Lynch, V. M.; Holliday, B. J.; Sessler, J. Copper selective polymeric extractant synthesized by ring-opening metathesis polymerization. *Inorg. Chem.* **2018**, *57* (1), 392–399.
- (21) Gandra, U. R.; Courjaret, R.; Machaca, K.; Al-Hashimi, M.; Bazzi, H. S. Multifunctional rhodamine B appended ROMP derived fluorescent probe detects Al3+ and selectively labels lysosomes in live cells. *Sci. Rep.* **2020**, *10* (1), 19519.
- (22) Shin, S.; Lim, J.; Gu, M.-L.; Yu, C.-Y.; Hong, M.; Char, K.; Choi, T.-L. Dimensionally controlled water-dispersible amplifying fluorescent polymer nanoparticles for selective detection of charge-neutral analytes. *Polym. Chem.* **2017**, *8* (48), 7507–7514.
- (23) Kovács, E.; Deme, J.; Turczel, G.; Nagy, T.; Farkas, V.; Trif, L.; Kéki, S.; Huszthy, P.; Tuba, R. Synthesis and supramolecular assembly of fluorinated biogenic amine recognition host polymers. *Polym. Chem.* **2019**, *10* (41), 5626–5634.
- (24) Ge, J. Z.; Liu, Z.; Cao, Q. Y.; Chen, Y.; Zhu, J. H. A Pyrene-functionalized Polynorbornene for Ratiometric Fluorescence Sensing of Pyrophosphate. *Chemistry - An Asian Journal* **2016**, *11* (5), 687–690.
- (25) Guo, Q.; Zhang, Y.; Lin, Z.-H.; Cao, Q.-Y.; Chen, Y. Fluorescent norbornene for sequential detection of mercury and biothiols. *Dyes Pigm.* **2020**, *172*, 107872.
- (26) Belger, C.; Weis, J. G.; Egap, E.; Swager, T. M. Colorimetric stimuli-responsive hydrogel polymers for the detection of nerve agent surrogates. *Macromolecules* **2015**, *48* (21), 7990–7994.

(27) Sha, S. C.; Zhu, R.; Herbert, M. B.; Kalow, J. A.; Swager, T. M. Chemical warfare simulant-responsive polymer nanocomposites: Synthesis and evaluation. *J. Polym. Sci., Part A: Polym. Chem.* **2017**, *55* (18), 3034–3040.

(28) Li, Y.; Chen, C.; Meshot, E. R.; Buchsbaum, S. F.; Herbert, M.; Zhu, R.; Kulikov, O.; McDonald, B.; Bui, N. T. N.; Jue, M. L.; Park, S. J.; Valdez, C. A.; Hok, S.; He, Q.; Doona, C. J.; Wu, K. J.; Swager, T. M.; Fornasiero, F. Autonomously Responsive Membranes for Chemical Warfare Protection. *Adv. Funct. Mater.* **2020**, *30* (25), 2000258.

(29) Vakalopoulou, E.; Borisov, S. M.; Slugovc, C. Fast Oxygen Scavenging of Macroporous Poly (Norbornadiene) Prepared by Ring-Opening Metathesis Polymerization. *Macromol. Rapid Commun.* **2020**, *41* (5), 1900581.

(30) Zhang, R.; Qin, X.; Kong, F.; Chen, P.; Pan, G. Improving cellular uptake of therapeutic entities through interaction with components of cell membrane. *Drug Delivery* **2019**, *26* (1), 328–342.

(31) Blum, A. P.; Yin, J.; Lin, H. H.; Oliver, B. A.; Kammeyer, J. K.; Thompson, M. P.; Gilson, M. K.; Gianneschi, N. C. Stimuli Induced Uptake of Protein-Like Peptide Brush Polymers. *Chemistry - A European Journal* **2022**, *28* (5), e202103438.

(32) Wei, G.; Su, Z.; Reynolds, N. P.; Arosio, P.; Hamley, I. W.; Gazit, E.; Mezzenga, R. Self-assembling peptide and protein amyloids: from structure to tailored function in nanotechnology. *Chem. Soc. Rev.* **2017**, *46* (15), 4661–4708.

(33) Blum, A. P.; Kammeyer, J. K.; Gianneschi, N. C. Activating peptides for cellular uptake via polymerization into high density brushes. *Chemical Science* **2016**, *7* (2), 989–994.

(34) Adamiak, L.; Touve, M. A.; LeGuyader, C. L. M.; Gianneschi, N. C. Peptide Brush Polymers and Nanoparticles with Enzyme-Regulated Structure and Charge for Inducing or Evading Macrophage Cell Uptake. *ACS Nano* **2017**, *11* (10), 9877–9888.